STRUCTURAL ANALYSIS IN DESIGNING CONICAL DISCS OF ROTATION

Perrin Smith Neto
Pontifícia Universidade Católica de Minas Gerais, Av. Dom José Gaspar,500,30535-610- Belo Horizonte
psmith@pucminas.br

Romulo Curzio Valente
Pontifícia Universidade Católica de Minas Gerais, Av. Dom José Gaspar,500,30535-610- Belo Horizonte
psneto@pucminas.br

Clovis Sperb de Barcellos
Pontifícia Universidade Católica de Minas Gerais, Av. Dom José Gaspar,500,30535-610- Belo Horizonte
clovis@pucminas.br

Marco Antonio Dutra Quinan
Centro de Desenvolvimento Tecnológico Nuclea/CNEN, R.Prof. Mario Werneck,sn/n, 30123-170,Belo Horizonte
quinan@cdtn.br

Abstract. *This study analyzes stress concentrations in symmetric and conical discs containing lateral holes and a 300mm external diameter, which goes round their own axis on a constant speed of 800 rpm. This value was taken as limit speed since it is capable of producing stresse lower then the elastic limits on over the piece for both normal and shear components. In order to allow a broader view of the results, conical discs with inclinations ranging from Oº to 45º were used, each of them with lateral holes varying in diameter from 15mm to 45m, totalizing 60 samples. The work aimed at understanding the correlation between disc inclination variation and stress concentration near lateral holes as well as the correlation between variation in lateral diameter and stress concentration near those holes. For such, models in a program of finite elements were designed and the results obtained from such models processed through analysis of statistical sensitivity. The results produced very clear conclusions which may serve as basis for the elaboration of future projects such as the one herein presented. The results obtained by the analysis of finite elements were also validated through a tri-dimensional photoelastic experimental technique which took as a model a disc with an inclination of 20º and lateral holes measuring 25mm, made from photoelastic resin. The result obtained from the photoelastic model proved to be very similar to that of its counterpart developed through the finite elements method. In order to determine disc profile conditions it was presumed that they rotated around a central axis measuring 25mm in diameter and that there was total restriction all over the contact surface between disc and axis. Finally, one must remark that the final objective of this study is to create conditions for the design of lighter discs capable of producing higher rotation speeds..*

Keywords*: conical discs, discs with holes, stress concentration,*discs with rotation

1. Introduction

Conical discs in rotation are structural elements of great application in turbine design to mechanical industry. Turbines give better efficiency and fuel economy. There are gas-turbine very used in central thermoelectric to generation of electrical energy. In this case, mainly rotational discs must have lateral holes to reduce weight and consequently permit more velocity of rotation once these rotors can work at great velocities. In many cases, rotation discs , medium surface is made conical to maintain an adequate axial distance between plates of turbine without increase length of central reinforcement and also to avoid more pressure difference through the length of discs. Due to great importance of stress analysis in rotational discs, special attention is given by researches and a lot of technical papers are devoted to this subject

Experimental stress analysis is a very efficient process that permits compare the obtained results by numerical and mathematics methods and relating both with physical system. (Knijnik ,1973) studied stress concentration induced by two non central holes in conical discs using photoelastic method. When considering a circular disc with central hole and uniform thickness rotating around it's simetric polar axis as figure 1, it can be shown that stress distribution is uniform through all thickness of the disc and it is a function of radial distance and velocity of rotation. For element ABCD , inertial force due to angular velocity ω $F_{INERTIAL} = (\gamma\omega^2 r^2/g)\, dr\, d\theta$.

Tangential and radial stress can be written as

$$\sigma_h = \frac{3+\nu}{8(1-\upsilon^2)} EN\left(r_1^{\ 2} + r_0^{\ 2} - \frac{1+3\nu}{3+\nu} r^2 + \frac{r_0^{\ 2} r_1^{\ 2}}{r^2} \right) \tag{1}$$

$$\sigma_r = \frac{3+\upsilon}{8(1-\upsilon^2)} EN\left(r_i^{\ 2} + r_0^{\ 2} - r^2 - \frac{r_1^{\ 2} r_0^{\ 2}}{r^2} \right) \tag{2}$$

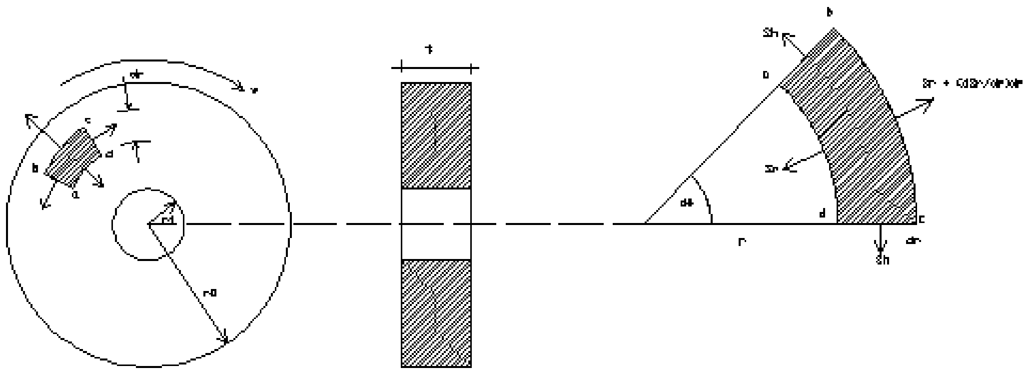

Figure 1 – Disc with rotation and inertial force

where maximum values are:

$$(\sigma_h)_{Max} = \frac{\gamma\omega^2 r_0^{\ 2}}{g}\left(\frac{3+\upsilon}{4}\right)\left(1 + \frac{1-\upsilon}{3+\upsilon}\frac{r_i^{\ 2}}{r_0^{\ 2}}\right) \tag{3}$$

$$(\sigma_r)_{Max} = \frac{\lambda\omega^2 r_0^{\ 2}}{g}\left(\frac{3+\nu}{8}\right)\left(1 - \frac{r_i}{r_0}\right)^2 \tag{4}$$

2.Geometry of discs

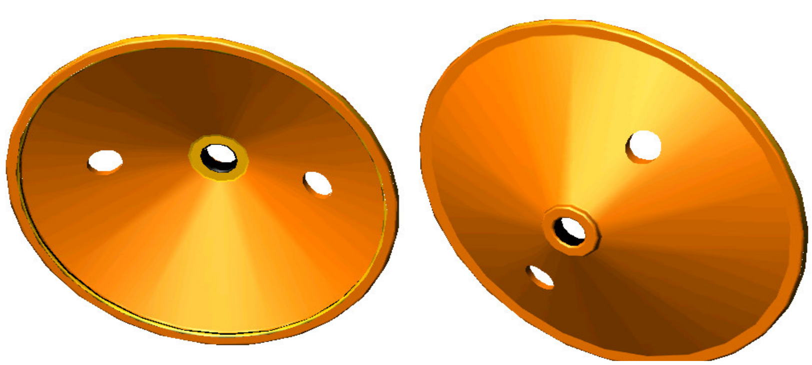

Figure 2. View of finite element discs

P

In finite element model idealized, all surface of contact of internal disc hole was in contact to an axis of rotation and our goal was to determine the stress concentration σ_r e σ_θ near non central holes once they were created to diminish weight of disc just to obtain a bigger velocity of rotation. In this paper our model reached ω = 1200 rpm . This rotation was capable of obtaining stress in a great spectrum without exceeding elastic limit of the material. To evaluate results of element finite models were used 30 units of rotational discs with inclination of medium surface with 6 different inclination, with angles of 0^0, 5^0 , 15^0, 25^0, 35^0 e 45^0 . For each inclination, six different discs were designed with non central holes of diameters: 15mm, 25mm, 35mm, 45mm e 55mm, maintaining the same central hole diameter of 25 mm. The surface of these discs were designed with variable thickness beginning with 5mm at external edge, until to 10 mm at internal edge. Also at each external and internal discs edge, reinforcement rings were designed of respectively 10x10 mm and 10x15mm. The reason of these reinforcement rings was to reduce the maximum effects of warping when these discs rotated around their axis.

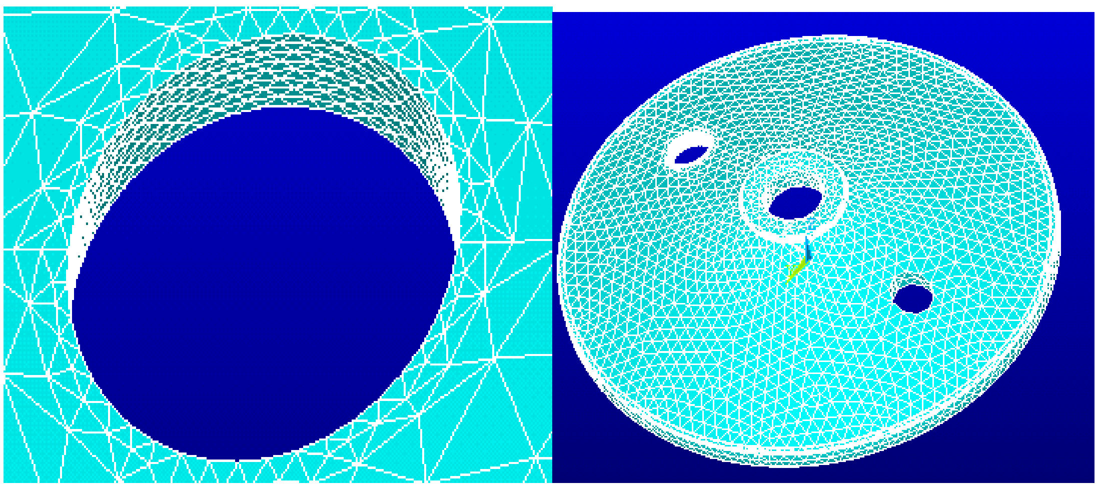

Figure 3– Numerical model developed using Ansys 7.1 software

Plane Disc
Cross section

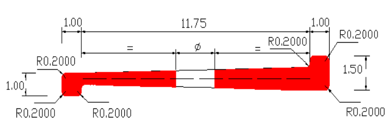

Inclined disc
Cross Section

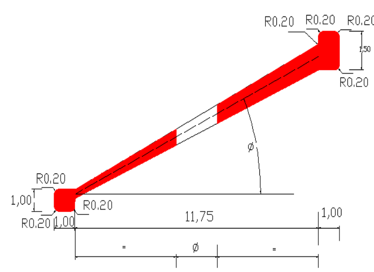

Figure 4– Cross section of plane discs

Figure 5 – Cross section of inclined discs

To comparison of results were created a photoelastic and a numerical model disc with 200mm of external diameter, 25 mm of central hole ,20 mm of lateral holes diameter and thickness varying from 0,4 to 0,5 mm.

3.Tridimensional Photoelasticity, slices and material

Tridimensional photoelaticity results obtained were used as parameters of comparison to validate final numerical results. Photoelastic material presents optic anisotropy in its interior, characterized by isoclinic and isochromatic fringes that are observed by monochromatic light effect. In each point isochromatic fringes are proportional to the difference of stress/strain in that point and isoclinic fringe gives direction of these stresses to a reference. Using three dimensional experimental photoelastic technique, according (Dally e Riley, 1991),models of epoxy resin were developed, loaded with rotation and finally that after cure, it was possible to slice and analyze stresses values in the point of study. The model observation was obtained in a transmission polariscope that gave parameters N (isochromatic fringe order) and ϕ (isoclinic fringe angle).

3.1. Load System

To obtain stresses and concentration stress factors by photoelasticity technique, it was built a load system. Figure 7 shows a first design of this project. Once tridimensional photoelasticity was used, a special system needed to be used to have disc inside an oven with controlled temperature. Figure 6 presents temperature and characteristics of epoxy resin used to this design.

Tc(^{0}C)- critical temperature	108^0
E (MPa) – elasticity modulus	9,58
fσ (N/m) – fringe order	0,026
Q(m^{-1}) – merit figure	368,46

Figure 6. Physical constants of photoelastic material at critical temperature

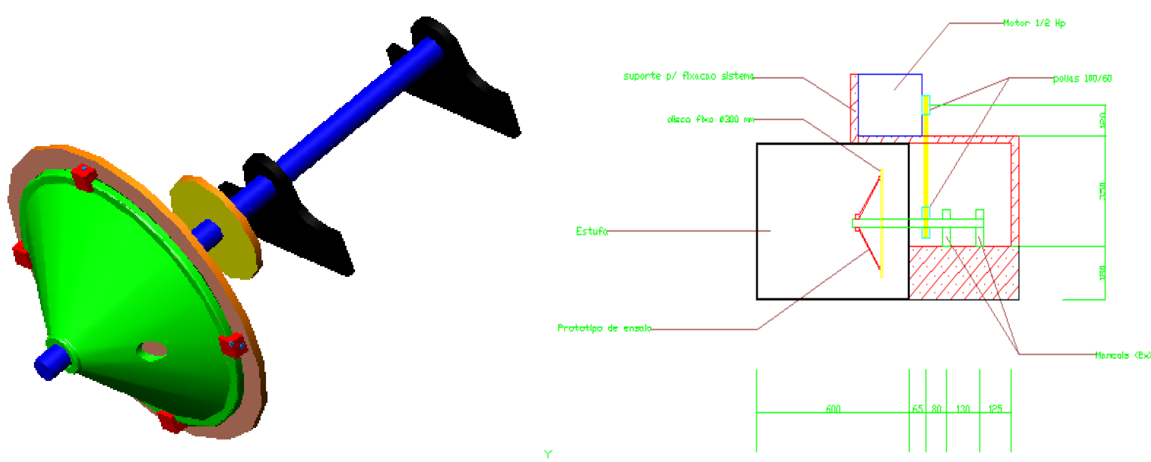

Figure 7- Designed load system to be adapted in a photoelastic oven

Load system used an electric motor with 2HP of power with a velocity of 1200 rpm, coupled to a shaft of rotating disc through pulley and belts as represented in figure 7. This rotating shaft was supported by two bearings. The conical disc was fixed at end supported by a plate whose purpose was to allow that during rotation there was no warping that could cause not desired stresses

Prototype Section

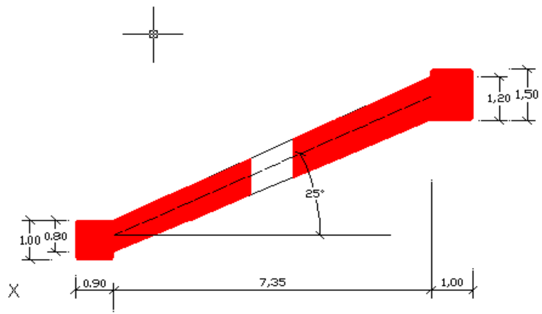

Figure 8– Section of disc used in photoelasticity to comparison

After cure process, both photoelastic discs were ready to slice and obtain stress values in points A and B, chosen for analysis(fig. 9 and 11). Next step after loading and stress freezing technique, slices of photoelastic material were cut in the interested planes to obtain stress analyses in polariscope. These slices show internal stress distribution in the chosen cut plane(fig. 10 and 11)

Figure 9 – Final machined model– inferior and superior view

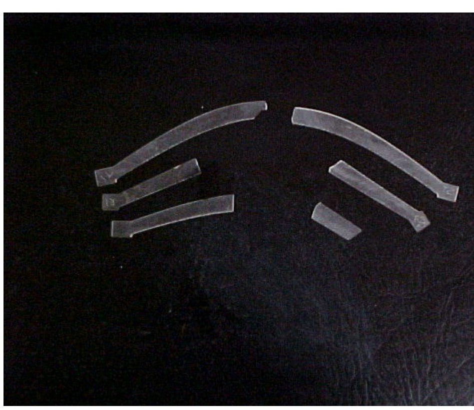

Figure 10 a- Slices of model cut after stress freezing

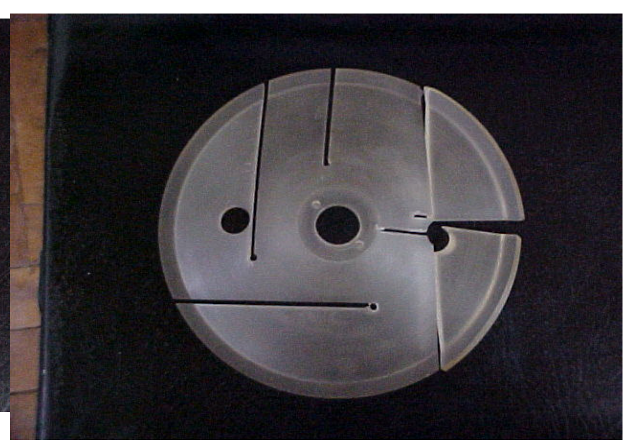

Figure 10 b– Cut disc made of photoelastic material

Next step after loading and stress freezing, slices of photoelastic material were cut in the interested planes to obtain stress analyses in polariscope. These slices show internal stress distribution in the chosen cut plane(fig. 10 and 11)

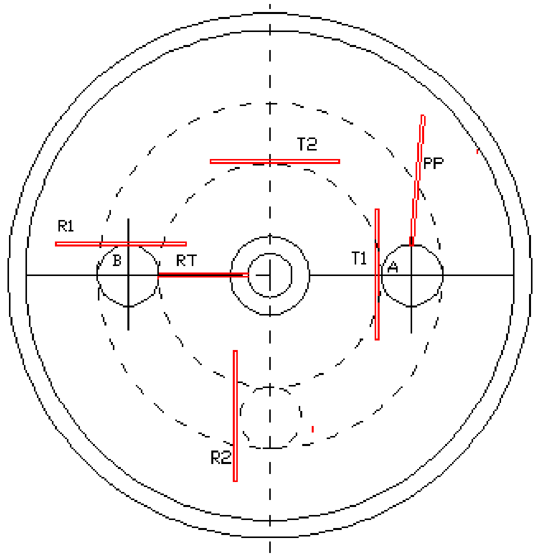

Figure 11 – Slices to be used in model

First slice was cut to evaluate was PP slice at line B. The unique stress component was σ_z. Using polariscope equipment, with light incident according radial direction, it was obtained:

$$(\sigma_z - \sigma_\theta)_B = \frac{N_{rB} * K}{t_{rB}} \qquad (5)$$

Where N_{rB} represents fringe order at considered point, measuring according direction r; t_{rB} represents thickness of slice A at considered point, belonging to line A, measured according direction r. This equation can be used in any point of line A where at this case $\sigma_{\theta A} = 0$ in any point of this line. As σ_{θ_R} =0, σ_{z_R} can be obtained directly. With this value, cutting slice A, and observing according direction θ, which will represent the difference of principal stress according line R.

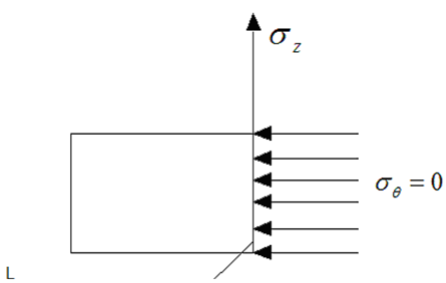

Figure 12 –stress at line B

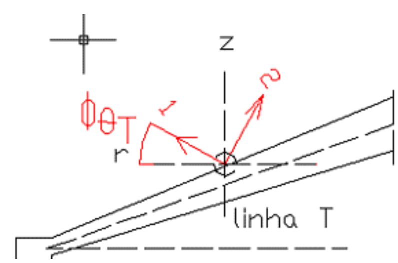

Figure 13- Stress at slice R

4.Comparison between numerical and photoelastic model

When stress in line B is analyzed, it can be seen that in both models, it moves from compression in the superior part to tension in the inferior part. In both models, the biggest stress is compression stress in superior part of line B.

Once radial stress in the superior point of line B increases with the introduction of hole, it is natural that the concentration stress coefficient increases also in superior part and decrease in inferior part.

Radial stress - numerical model			
Layer	Solid Disc	Bored Disc	Concentration Factor
Superior	-60	-148	2,47
Inferior	80	46	0,58
Radial stress - photoelastic model			
Layer	Solid Disc	Bored Disc	Concentration Factor
Superior	-89	-200	2,25
Inferior	80	46	0,52

Figure 11- Radial stress and stress concentration in

Tangential stress - numerical model			
Layer	Solid Disc	Bored Disc	Concentration Factor
Superior	35	21	0,6
Inferior	165	378	2,29
Tangential stress - photoelastic model			
Layer	Solid Disc	Bored Disc	Concentration Factor
Superior	88	84	0,71
Inferior	44	119	2,7

Figure12 - Tangential stress and stress concentration in A

When analyzing tangential stress in line A, it can be seen that in both models, it is always of tension both in superior and in inferior part. In both models, maximum stress occurs in inferior part of line A. Tangential stress occurs in line A. Tangential stress in inferior point of figure A was the smaller stress found in this research

5. Results obtained in both numerical and photoelastic models

Using only one comparative model, results indicated in figures 11 and 12 show that stress concentration factor found both in tangential and radial stress are very closed validating the test. Mesh refinement in sub regions of stress concentration, previously chosen in such refinement, bring to a better description of stress concentration in these models when used such technique to compare both models.
a) Stress concentration in point A of inferior face
In all discs it was observed that as lateral hole diameters increased stress concentration coefficient also increased. Positive values found to these coefficients indicate that stresses didn't change signal in any case.
Discs with 25^o inclination, with increase of lateral hole diameters, stress concentration factors increased in a more smooth way. Disc inclusive and above 35^o inclination, an increase of lateral hole diameters, produced a very increase expressive increase in stress concentration factors. As example, it was observed that discs with 45^o inclination and lateral hole with 55 mm diameter a value of 6 was obtained to stress concentration factor, which in practice corresponds to a stress near elastic limit.
b) Stress concentration in point B of inferior face.
Concentration stress factors changed signal as inclination of discs increased, indicating that in a determined point these stresses turned from tension to compression. To discs with until 5^o inclination all stress cocentration factors although decreasing presented positive value.Above 25^0 inclination and lateral hole diameter of 35 mm, factors changed signal-indicating occurrence of compression stresses.
c) Stress concentration in point A of superior face. Although bigger stress occur at point A of inferior face, it was observed that in discs with inclination of 35^o or more, concentration stress factors presented high values around 3,5 near lateral holes with diameter of 15 mm and value of 1,5 closed lateral holes of 55 mm of diameter;
d) Stress concentration in point B of superior face. All concentration coefficients are positive indicating that there was no reversion in stress with introduction of lateral holes.
e) At lateral holes with 1,5 cm diamter, these stress concentration factors remained aroung 2, with value between 1 and 2 at lateral holes with diameter of 5,5 cm.

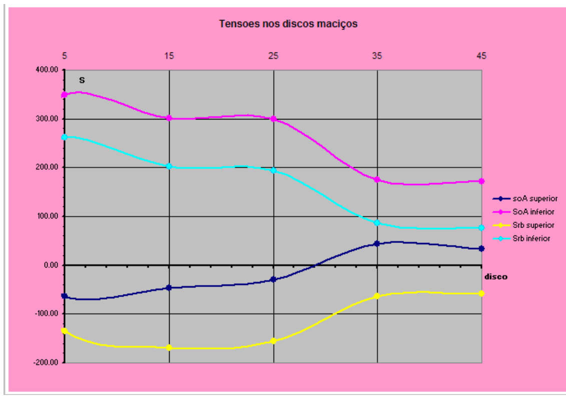

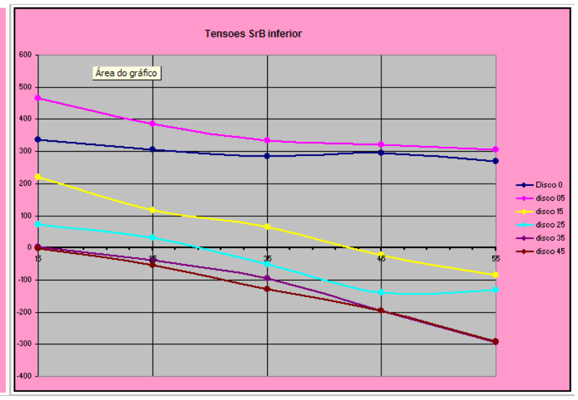

Figure 13 –Inferior radial stress at B section at solid Discs versus variation of lateral holes

Figure 14- Radial and tangential stress at solid discs versus disc angle inclination

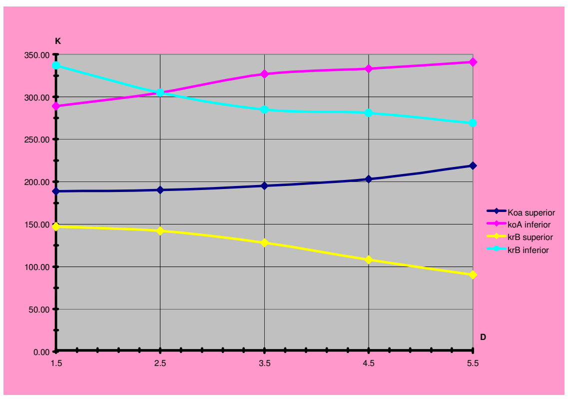

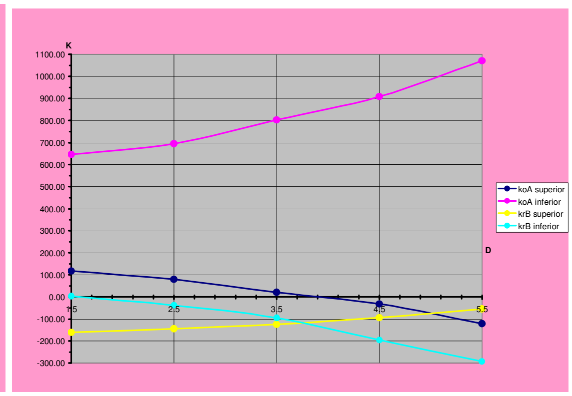

Figure 15 – Disc with 0^0 inclination- radial and tangential stress x lateral hole variation

Figure 16- Disc with 35^0 inclination- radial and tangential stress versus lateral hole variation

6. Acknowledgements

The authors gratefully acknowledge the Conselho Nacional de Desenvolvimento Científico e Tecnológico (CNPq) and Fundação de Auxilio à Pesquisa do Estado de Minas Gerais (FAPEMIG) at Brazil for its joint support of this research.

7. References

Dally, J, W., and Riley, W, F., 1965, “Experimental Stress Analysis ” , Mc-Graw-Hill .

Durelli, A, J. and Riley, W, F.,1965, “Introdution to photomechanics ” , Prentice-Hall

Edward J. Haug, et all ,1986, “Design Sensitivity Analisys of Structural Systems”, Academic Press Inc.

Fessler, H. and Thorpe, T, E.,1967, “Optimization of stress concentration at holes in rotating discs”, J. Strain Analysis ,n^0 2, pag 152.

Green, W, A. and Hetherington, R,. 1964, “Stress distribution in rotation discs witch non central holes ”, Aro. Quart , $n^0$15, pag.107

Leven, M, M. and Sampson, R, C.,1956 “ Large epoxi resin casting for three-dimensional photoelastic tests”. Res. Rept., 60-94459-2-R3, Westinghouse Research laboratories.

Knijnik, A., (1972) , “Concentração de tensões introduzidas por dois furos não centrais em discos cônicos de rotação usando o método fotoelástico. ”, tese de Mestrado , UFRGS

8. Responsibility notice

The authors are the only responsible for the printed material included in this paper.